

# Reynolds Averaged Navier-Stokes Flow Computation of RAE2822 Airfoil Using Gas-kinetic BGK Scheme

Ong J. Chit, Ashraf A. Omar, and Waqar Asrar

**Abstract**— In this paper, a gas-kinetic solver is developed to solve Reynolds Averaged Navier-Stokes (RANS) equations in two-space dimensions generalized coordinates. The convection flux terms which appear on the left hand side of the RANS equations are discretized by a semi-discrete finite difference method. Then, the resulting inviscid flux functions are approximated by gas-kinetic BGK scheme which is based on the BGK model of the approximate collisional Boltzmann equation. The cell interface values required by the inviscid flux functions are reconstructed to second-order spatial accuracy via the MUSCL (Monotone Upstream-Centered Schemes for Conservation Laws) variable interpolation method coupled with a minmod limiter. As for the diffusion flux terms, they are discretized by a second-order central difference scheme. To account for the turbulence effect, a combined  $k-\varepsilon$  /  $k-\omega$  SST (Shear-Stress Transport) two-equation turbulence model is used in the solver. An explicit-type time integration method known as the modified fourth-order Runge-Kutta method is used to march the solution to steady-state. Computation over the RAE2822 airfoil flow corresponding to transonic speed has been solved using the developed gas-kinetic solver. Accuracy of BGK scheme in solving viscous transonic turbulent flow over the airfoil will be examined. Results obtained from the computations are also compared with experimental data and will demonstrate that a very good agreement has been achieved.

**Index Terms**—BGK scheme, compressible turbulent flow, finite difference method, high-order accuracy, transonic airfoil.

## I. INTRODUCTION

Throughout the history of computational fluid dynamics development, many numerical schemes have been created to solve practical application of gas dynamics. The key design criterion of any numerical schemes is to maximize robustness and accuracy. This requirement is particularly important in compressible flows involving high-speed flow where intense shock waves and boundary layers may simultaneously exist. Among those notable and successful are the Godunov-type and flux vector splitting schemes. Besides these numerical

schemes that stem from the discretization of the convective terms, the gas-kinetic schemes have attracted much attention in recent years due to their high robustness and accuracy.

Recent developments have seen the emergence of another class of scheme known as the gas-kinetic schemes that are developed based on the Boltzmann equation [1], [2]. Mainly, there are two groups of gas-kinetic schemes and the difference lies within the type of Boltzmann equation use in the gas evolution stage. One of them is the well-known KFVS (Kinetic Flux Vector Splitting) scheme which is based on the collisionless Boltzmann equation and the other is based on the collisional BGK (Bhatnagar-Gross-Krook) model [3] where the BGK scheme is derived. Like any other FVS method, the KFVS scheme is very diffusive and less accurate in comparison with the Roe-type FDS method. The diffusivity of the FVS schemes is mainly due to the particle or wave-free transport mechanism, which sets the CFL time step equal to particle collision time [4]. In order to reduce diffusivity, particle collisions have to be modeled and implemented into the gas evolution stage. One of the distinct approaches to take particle collision into consideration in gas evolution can be found in [1]. In this method, the collision effect is considered by the BGK model as an approximation of the collision integral in the Boltzmann equation. It is found that this gas-kinetic BGK scheme possesses accuracy that is superior to the flux vector splitting schemes and avoids the anomalies of FDS-type schemes [5]-[9].

Turbulent flow motions occur in vast majority of fluid applications. To name a few: fluid flow in a pipe, flow processes in combustion chamber and even flow over an airfoil will exhibit a chaotic complex motion defined as turbulent flow. The most elegant solution to any turbulent flow is via the Direct Numerical Simulation (DNS) of turbulence. This approach is implemented by discretizing the Navier-Stokes equations with higher order accurate numerical scheme and solved using extremely fine grid mesh. An alternative approach to the DNS technique would be the adoption of Large Eddy Simulation (LES), which draws the advantages of the direct simulation of turbulence flows and the solution of the Reynolds averaged equations through closure assumptions. Although the popularity of DNS and LES have become noticeable [10]-[12] due to rapid development of high performance computing technology, the general trend of computing turbulent flows still remain with the solution of Reynolds-Averaged Navier-Stokes (RANS) equations with the inclusion of Reynolds stresses into the original full Navier-Stokes equations. Resolving the

Manuscript received November 10, 2008. This work was supported by International Islamic University Malaysia (IIUM) through Research Management Center under the grant No. EWD B-0703-32.

Ong J. Chit is with the Department of Mechanical Engineering, International Islamic University Malaysia, Kuala Lumpur 50728 Malaysia (e-mail: jchitong@yahoo.com).

Ashraf A. Omar is with the Department of Mechanical Engineering, International Islamic University Malaysia, Kuala Lumpur 50728 Malaysia (phone: +60361964486; fax: +60361964455; e-mail: aao@iiu.edu.my).

Waqar Asrar is with the Department of Mechanical Engineering, International Islamic University Malaysia, Kuala Lumpur 50728 Malaysia (e-mail: waqar@iiu.edu.my).

turbulent flows via this means proved to be computationally cheaper [13], [14]. The closure equations that provide the additional Reynolds stresses in the RANS equations are calculated from turbulence models.

In the present work, a flow solver based on the gas-kinetic BGK scheme is developed and tested. The BGK scheme is used to approximate the convective flux terms, while a second-order central scheme is used to discretize the diffusive flux terms of the RANS equations, coupled with a combined k-ε / k-ω SST two-equation turbulence model to provide the required Reynolds stresses to resolve the turbulent flow. The numerical solver is tested with a transonic flow over a RAE2822 airfoil according to the AGARD test case 9 in order to assess its computational capabilities. The computed results are compared with existing experimental data taken from [15] and demonstrated that a very good agreement is obtained.

## II. NUMERICAL METHODS

The two-dimensional normalized Reynolds-averaged Navier-Stokes equations in the computational space can be written in strong conservation form as

$$\frac{\partial \bar{W}}{\partial t} + \frac{\partial \bar{F}}{\partial \xi} + \frac{\partial \bar{G}}{\partial \eta} = \frac{\partial \bar{F}_v}{\partial \xi} + \frac{\partial \bar{G}_v}{\partial \eta}$$

where

$$\bar{W} = \frac{1}{J} \begin{bmatrix} \rho \\ \rho U \\ \rho V \\ \rho \varepsilon \end{bmatrix}, \bar{F} = \frac{1}{J} \begin{bmatrix} \xi_x (\rho U) + \xi_y (\rho V) \\ \xi_x (\rho U^2 + p) + \xi_y (\rho UV) \\ \xi_x (\rho UV) + \xi_y (\rho V^2 + p) \\ \xi_x (\rho \varepsilon U + pU) + \xi_y (\rho \varepsilon V + pV) \end{bmatrix},$$

$$\bar{G} = \frac{1}{J} \begin{bmatrix} \eta_x (\rho U) + \eta_y (\rho V) \\ \eta_x (\rho U^2 + p) + \eta_y (\rho UV) \\ \eta_x (\rho UV) + \eta_y (\rho V^2 + p) \\ \eta_x (\rho \varepsilon U + pU) + \eta_y (\rho \varepsilon V + pV) \end{bmatrix},$$

$$\bar{F}_v = \frac{1}{J} \begin{bmatrix} 0 \\ \xi_x \tau_{xx} + \xi_y \tau_{xy} \\ \xi_x \tau_{xy} + \xi_y \tau_{yy} \\ \xi_x (U \tau_{xx} + V \tau_{xy} - q_x) + \xi_y (U \tau_{xy} + V \tau_{yy} - q_y) \end{bmatrix},$$

$$\bar{G}_v = \frac{1}{J} \begin{bmatrix} 0 \\ \eta_x \tau_{xx} + \eta_y \tau_{xy} \\ \eta_x \tau_{xy} + \eta_y \tau_{yy} \\ \eta_x (U \tau_{xx} + V \tau_{xy} - q_x) + \eta_y (U \tau_{xy} + V \tau_{yy} - q_y) \end{bmatrix}$$

With  $\rho$ ,  $U$ ,  $V$ ,  $p$  and  $\varepsilon$  are the macroscopic density, x-component of velocity, the y-component of velocity, the pressure and total energy, respectively. While,  $\tau_{xx}$ ,  $\tau_{xy}$ ,  $\tau_{yy}$  are the shear stress terms and  $q_x$ ,  $q_y$  are the heat conduction terms along the x- and y-directions, respectively. A detailed description about the viscous shear stresses appearing in the above equations can be found in [16].

From the perspective of RANS computation, the viscosity  $\mu$  in the stress terms and the term  $(\mu / Pr)$  in the heat conduction terms are modeled as

$$\mu = \mu_l + \mu_t$$

$$\frac{\mu}{Pr} = \left( \frac{\mu}{Pr} \right)_l + \left( \frac{\mu}{Pr} \right)_t$$

where the subscripts l and t represent laminar and turbulent contributions, respectively. The parameter  $(Pr)_t$  is called the turbulent Prandtl number and for air it is generally taken to be 0.9 for wall bounded flows. The closure model chosen to yield the turbulent viscosity  $\mu_t$  that appears in the RANS equations is the combined k-ε / k-ω SST two-equation turbulence model which is given as

$$\frac{\partial}{\partial t} (\rho k) + \frac{\partial}{\partial x_j} (\rho u_j k) = \frac{\partial}{\partial x_j} \left[ (\mu + \sigma_k \mu_t) \frac{\partial k}{\partial x_j} \right] + P_k - \beta^* \rho \omega k \quad (3)$$

$$\begin{aligned} \frac{\partial}{\partial t} (\rho \omega) + \frac{\partial}{\partial x_j} (\rho u_j \omega) = & \frac{\partial}{\partial x_j} \left[ (\mu + \sigma_\omega \mu_t) \frac{\partial \omega}{\partial x_j} \right] \\ & + 2(1 - F_1) \rho \sigma_{\omega 2} \frac{1}{\omega} \frac{\partial k}{\partial x_j} \frac{\partial \omega}{\partial x_j} \\ & + \alpha \frac{\omega}{k} P_k - \beta \rho \omega^2 \end{aligned} \quad (4)$$

where the production of turbulence  $P_k$  is defined as

$$P_k = \left[ \mu_t \left( \frac{\partial u_i}{\partial x_j} + \frac{\partial u_j}{\partial x_i} - \frac{2}{3} \delta_{ij} \frac{\partial u_k}{\partial x_k} \right) - \frac{2}{3} \rho k \delta_{ij} \right] \frac{\partial u_i}{\partial x_j} \quad (5)$$

The closure constants used in the preceding equations are outlined clearly in [17].

(1) A standard BGK scheme is based on the collisional Boltzmann equation and it is written in two dimensions as [1]

$$\frac{\partial f}{\partial t} + u \frac{\partial f}{\partial x} + v \frac{\partial f}{\partial y} = \frac{(g - f)}{\tau} \quad (6)$$

where  $f$  is the real particle distribution function and  $g$  is the equilibrium state approached by  $f$  within a collision time scale  $\tau$ . Both  $f$  and  $g$  are functions of space  $x$ ,  $y$ ; time  $t$ ; particle velocity  $u$ ,  $v$ ; and internal degrees of freedom  $\zeta$ . The equilibrium state  $g$  in the 2D BGK model is the Maxwell-Boltzmann distribution function and it has the following form

$$g = \rho \left( \frac{\lambda}{\pi} \right)^{(K+2)/2} e^{-\lambda [(u-U)^2 + (v-V)^2 + \zeta^2]} \quad (7)$$

where  $\lambda$  is a function of density and pressure,  $\lambda = \rho / 2p$ .  $\zeta$  is a  $K$  dimensional vector which accounts for the internal degrees of freedom such as molecular rotation, translation and vibration. The dimensional vector,  $K$  is related to the specific heat ratios and the space dimension by the relation  $K = (4 - 2\gamma) / (\gamma - 1)$ , where for a diatomic gas  $\gamma = 1.4$ . The relations between the densities of mass  $\rho$ , momentum  $(\rho U, \rho V)$ , and total energy  $\varepsilon$  with the distribution function  $f$  are derived from the following moment relation

$$\begin{pmatrix} \rho \\ \rho U \\ \rho V \\ \varepsilon \end{pmatrix} = \int f \Psi d\Xi \quad (8)$$

where  $d\Xi = dudvd\zeta$  is the volume element in the phase space while  $\Psi$  is the vector of moments given as

$$\Psi = \begin{pmatrix} 1 \\ u \\ v \\ \frac{1}{2} (u^2 + v^2 + \zeta^2) \end{pmatrix} \quad (9)$$

(2) With the moment relation defined in (8), a similar approach could be adopted in obtaining the numerical fluxes across cell interfaces and they are given as

$$F_x = \int u f \Psi d\Xi \quad (10)$$

$$G_y = \int v f \Psi d\Xi$$

where  $F_x$  and  $G_y$  are the physical flux in the x- and y-direction, respectively. A general solution for  $f$  of (7) at the cell interface  $(x_{i+1/2}, y_j)$  in two dimensions is obtained as [7]

$$f(0,0,t,u,v,\zeta) = (1-\phi)g_o + \phi f_o(-ut, -vt) \quad (11)$$

where  $\phi = e^{-\tau}$  is an adaptive parameter. For a first-order scheme  $\phi$  can be fixed in the numerical calculations. When the BGK scheme is extended to high-order, the value of  $\phi$  should depend on the real flow situations. Finally, the gas-kinetic BGK numerical flux across the cell interface in the x-direction can be computed as

$$F_x = \int u f(0,0,t,u,v,\zeta) \Psi d\Xi \quad (12)$$

$$F_x = (1-\phi)F_x^e + \phi F_x^f$$

where  $F_x^e$  is the equilibrium flux function and  $F_x^f$  is the non-equilibrium or free stream flux function. Hence, the numerical flux for the BGK scheme at the cell interface in the x-direction are obtained from (12) as

$$F_{i+1/2,j} = (1-\phi)F_{i+1/2,j}^e + \phi F_{i+1/2,j}^f \quad (13)$$

While the numerical flux at the cell interface in the y-direction is obtained in a similar manner and the resulting relation is presented as

$$G_{i,j+1/2} = (1-\phi)G_{i,j+1/2}^e + \phi G_{i,j+1/2}^f \quad (14)$$

In extending the numerical scheme to high-order spatial accuracy, the MUSCL approach [18] is adopted together with the minmod limiter. Hence, the left and right states of the primitive variables  $\rho$ ,  $U$ ,  $V$ ,  $p$  at a cell interface could be obtained through the non-linear reconstruction of the respective variables and are given as

$$Q_l = Q_{i,j} + \frac{1}{2} \phi \left( \frac{\Delta Q_{i+1/2,j}}{\Delta Q_{i-1/2,j}} \right) \Delta Q_{i-1/2,j} \quad (15)$$

$$Q_r = Q_{i+1,j} - \frac{1}{2} \phi \left( \frac{\Delta Q_{i+3/2,j}}{\Delta Q_{i+1/2,j}} \right) \Delta Q_{i+1/2,j}$$

where  $Q$  is a primitive variable and the subscript l, and r correspond to the left and right side of a considered cell interface. In addition,  $\Delta Q_{i+1/2,j} = Q_{i+1,j} - Q_{i,j}$ . The minmod limiter used in the reconstruction of flow variables in (15) is given as

$$\phi(\Omega) = \min \text{mod}(1, \Omega) = \max[0, \min(1, \Omega)] \quad (16)$$

For the time integration of steady state problems, an explicit formulation is chosen for the current solver which utilizes a fourth-order Runge-Kutta method. Applying this method to the generalized two-dimensional RANS equations provides the following results

$$\begin{aligned} \bar{W}_{i,j}^{(1)} &= \bar{W}_{i,j}^n \\ \bar{W}_{i,j}^{(2)} &= \bar{W}_{i,j}^n - \frac{\Delta t}{4} \left[ \left( \frac{\partial \bar{F}}{\partial \xi} \right)_{i,j}^{(1)} + \left( \frac{\partial \bar{G}}{\partial \eta} \right)_{i,j}^{(1)} - \left( \frac{\partial \bar{F}_v}{\partial \xi} \right)_{i,j}^{(1)} - \left( \frac{\partial \bar{G}_v}{\partial \eta} \right)_{i,j}^{(1)} \right] \\ \bar{W}_{i,j}^{(3)} &= \bar{W}_{i,j}^n - \frac{\Delta t}{3} \left[ \left( \frac{\partial \bar{F}}{\partial \xi} \right)_{i,j}^{(2)} + \left( \frac{\partial \bar{G}}{\partial \eta} \right)_{i,j}^{(2)} - \left( \frac{\partial \bar{F}_v}{\partial \xi} \right)_{i,j}^{(2)} - \left( \frac{\partial \bar{G}_v}{\partial \eta} \right)_{i,j}^{(2)} \right] \\ \bar{W}_{i,j}^{(4)} &= \bar{W}_{i,j}^n - \frac{\Delta t}{2} \left[ \left( \frac{\partial \bar{F}}{\partial \xi} \right)_{i,j}^{(3)} + \left( \frac{\partial \bar{G}}{\partial \eta} \right)_{i,j}^{(3)} - \left( \frac{\partial \bar{F}_v}{\partial \xi} \right)_{i,j}^{(3)} - \left( \frac{\partial \bar{G}_v}{\partial \eta} \right)_{i,j}^{(3)} \right] \\ \bar{W}_{i,j}^{n+1} &= \bar{W}_{i,j}^n - \Delta t \left[ \left( \frac{\partial \bar{F}}{\partial \xi} \right)_{i,j}^{(4)} + \left( \frac{\partial \bar{G}}{\partial \eta} \right)_{i,j}^{(4)} - \left( \frac{\partial \bar{F}_v}{\partial \xi} \right)_{i,j}^{(4)} - \left( \frac{\partial \bar{G}_v}{\partial \eta} \right)_{i,j}^{(4)} \right] \end{aligned} \quad (17)$$

### III. RESULTS AND DISCUSSIONS

The transonic flow over RAE2822 airfoil test case is selected in order to demonstrate the application of the developed BGK flow solver incorporated with a turbulence model (i.e. combined k- $\epsilon$  / k- $\omega$  SST). Extensive experimental data are available for this airfoil (i.e. [15], [19], [20]), thus making it an ideal test case for validating the computed results.

In this test case, flow conditions corresponding to AGARD test case 9 are used, namely, Mach number  $M_\infty = 0.73$ , Reynolds number  $Re_\infty = 6.5 \times 10^6$  and angle of attack  $\alpha = 2.8^\circ$ . The free stream conditions used for initializing the flow domain are specified as: density  $\rho_\infty = 1.486 \text{ kg/m}^3$ , temperature  $T_\infty = 255.6 \text{ K}$  and reference length  $L_\infty = 0.3048 \text{ m}$ . A structure C-grid with dimensions of 369 by 65 is generated by an algebraic grid generation method and is shown in zoom in view in Fig. 1. As for the specification of conditions along the boundaries, the following are enforced: viscous wall boundary condition is applied at the airfoil surface; averaging boundary condition is used along the wake cut to provide continuous flow variables; free stream condition is applied at the outer boundary; the boundaries located on the right are applied with outflow condition where static pressure is fixed to the free stream pressure.

The computed pressure contours are shown in Fig. 2, which predicts a shock-boundary layer interaction occurring at location about 60% of chord length on the upper surface of the airfoil. The computed pressure distribution is compared with the experimental data extracted from [15] in Fig. 3. The results illustrated in the figure show that the rooftop pressure is accurately resolved and the pressure recovery which occurs after the shock is well predicted with remarkable accuracy. However, the shock location is slightly predicted down stream in comparison to the experimental data. For viscous flow computation, it is always useful to examine how well the skin friction coefficient along the surface is resolved. Hence, the computed skin friction coefficient distribution along the airfoil surface is compared with experimental data from [15] in Fig. 4. The resolution of the skin friction coefficient on the upstream side of the shock location on the top side of the airfoil surface is predicted with great accuracy. In addition, the skin friction coefficient is slightly over-predicted in the region after the shock. No detailed comment can be made with regards to the skin friction coefficient on the bottom side of the airfoil surface because

there is just one experimental data point available in that region.

#### IV. CONCLUSION

A numerical solver based on the collisional BGK model of the Boltzmann equation has been successfully developed to simulate two-dimensional compressible turbulent flow based on the Reynolds-Averaged Navier-Stokes equations which utilizes a combined  $k-\epsilon$  /  $k-\omega$  SST turbulence model to provide the turbulent eddy viscosity. A transonic flow over a RAE2822 airfoil is selected in the current study to assess the numerical capabilities of this solver in computing compressible turbulent flow. The computed results for this test case clearly demonstrate that the BGK scheme is able to provide an accurate resolution of the flow, good prediction of shock location and remarkable post shock recovery of flow variables. These claims are justified by comparisons of the numerical findings of the BGK scheme with existing experimental data via examining the relevant flow properties such as pressure contours, pressure coefficient and skin friction coefficient.

#### REFERENCES

- [1] K. Xu, "Gas-Kinetic Scheme for Unsteady Compressible Flow Simulations," Von Kármán Ins. for Fluid Dynamics Lecture Series, vol. 1998-03, Von Kármán Ins., Rhode St. Genese, Belgium, 1998.
- [2] J. C. Ong, "Computational Analysis of Gas-Kinetic BGK Scheme for Inviscid Compressible Flow," M. Sc. Thesis, University Putra Malaysia, Malaysia, 2004.
- [3] J. C. Ong, A. A. Omar, W. Asrar, and M. M. Hamdan, "Development of Gas-Kinetic BGK Scheme for Two-Dimensional Compressible Inviscid Flows," AIAA Paper 2004-2708, 2004.
- [4] K. Xu, "Gas-Kinetic Theory Based Flux Splitting Method for Ideal Magnetohydrodynamics," ICASE Report, 98-53, Nov. 1998.
- [5] D. S. Chae, C. A. Kim, and O. H. Rho, "Development of an Improved Gas-Kinetic BGK Scheme for Inviscid and Viscous Flows," Journal of Computational Physics, vol. 158, pp. 1-27, 2000.
- [6] J. C. Ong, A. A. Omar, and W. Asrar, "Evaluation of Gas-Kinetic Schemes for 1D Inviscid Compressible Flow Problem," International Journal of Computational Engineering Science (IJCES), vol. 4, no. 1, pp. 829-851, Dec. 2003.
- [7] J. C. Ong, A. A. Omar, W. Asrar, and M. M. Hamdan, "An Implicit Gas-Kinetic BGK Scheme for Two-Dimensional Compressible Inviscid Flows," AIAA Journal, vol. 42, no. 7, pp 1293-1301, 2004.
- [8] J. C. Ong, A. A. Omar, W. Asrar, and Z. A. Zaludin, "Gas-Kinetic BGK Scheme for Hypersonic Flow Simulation," AIAA Paper, 2006-0990, Jan. 2006.
- [9] S. N. Adduslam, J. C. Ong, M. M. Hamdan, A. A. Omar, and W. Asrar, "Application of Gas-Kinetic BGK Scheme for Solving 2-D Compressible Inviscid Flow around Linear Turbine Cascade," Int. Journal for Computational Methods in Engineering Science and Mechanics, vol. 7, no. 6, Nov. 2006.
- [10] A. Leonard, "Energy Cascade in Large-Eddy Simulations of Turbulent Fluid Flows," Advances in Geophysics, vol. 18A, pp. 237-248, 1974.
- [11] Z. Liu, W. Zhao, and C. Liu, "Direct Numerical Simulation of Transition in a Subsonic Airfoil Boundary Layer," AIAA-97-0752, January, 1997.
- [12] F. F. Hatay, and S. Biringen, "Direct Numerical Simulation of Low-Reynolds Number Supersonic Turbulent Boundary Layers," AIAA-95-0581, January, 1995.
- [13] K. C. Ng, M. Z. Yusoff, and T. F. Yusaf, "Simulations of Two-Dimensional High Speed Turbulent Compressible Flow in a Diffuser and a Nozzle Blade Cascade," American Journal of Applied Sciences 2 (9), pp. 1325-1330, 2005.
- [14] N. J. Georgiadis, J. E. Drummond, and B. P. Leonard, "Evaluation of Turbulence Models in the PARC Code for Transonic Diffuser Flows," AIAA-94-0582, January, 1994.
- [15] Lien, F.S.; Kalitzin, G.; and Durbin, P.A.; "RANS modeling for compressible and transitional flows," Center for Turbulence Research summer proceedings, pp. 267-286, 1998.

- [16] K. A. Hoffmann, and S. T. Chiang, "Computational Fluid Dynamics for Engineers," Engineering Education System, Wichita, vol. 2, chap. 11 and 14, 1993.
- [17] K. A. Hoffmann, and S. T. Chiang, "Computational Fluid Dynamics for Engineers," Engineering Education System, Wichita, vol. 3, chap. 21, 2000.
- [18] C. Hirsch, "The Numerical Computation of Internal and External Flows," John Wiley & Sons, New York, vol. 2, chap. 21, 1990.
- [19] J. W. Slater, "RAE2822 Transonic Airfoil: Study #1," NASA Glenn Research Centre, Ohio. Internet: <http://www.grc.nasa.gov/WWW/wind/valid/raetaf/raetaf01/raetaf01.html>
- [20] J. P. Singh, "An improved Navier-Stokes flow computation of AGARD Case-10 flow over RAE2822 airfoil using Baldwin-Lomax model," Acta Mechanica, vol. 151, pp. 255-263, 2001.

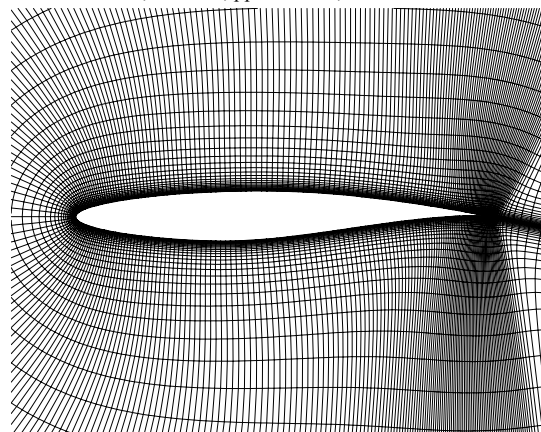


Fig. 1: RAE2822 airfoil computational mesh, 369 x 65.

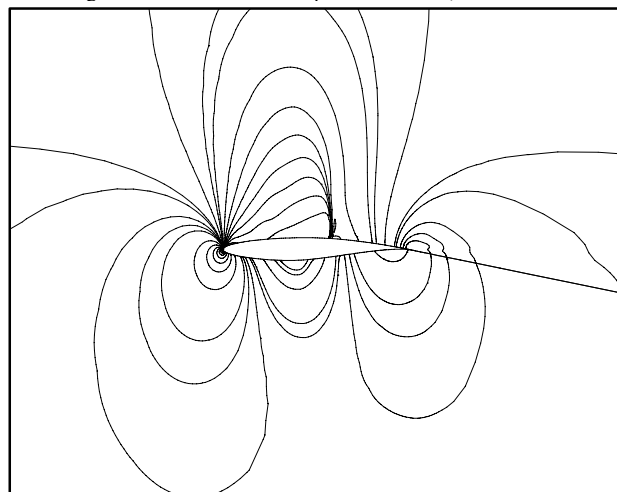


Fig. 2: Pressure contours near the RAE2822 transonic airfoil.

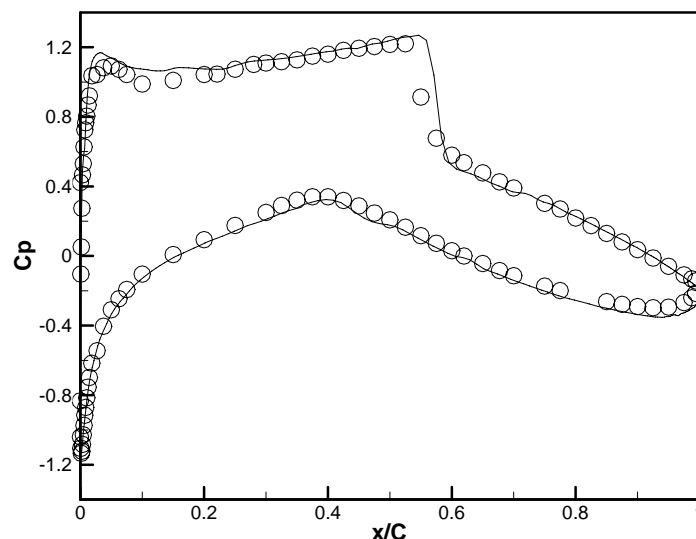


Fig. 3: Pressure coefficient distribution on the RAE2822 airfoil: BGK scheme —, experiment O.

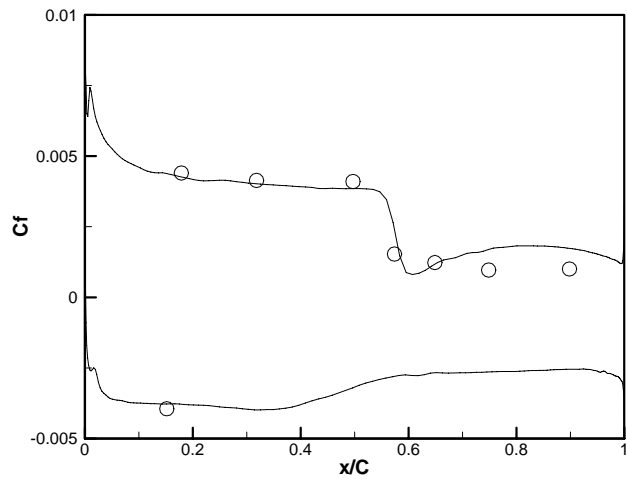


Fig. 4: Skin friction coefficient distribution on the RAE2822 airfoil: BGK scheme —, experiment O.